Flechtner, F., Neumayer, K.-H., Dahle, C., Dobslaw, H., Fagiolini, E., Raimondo, J.-C., Güntner, A. (2016): What Can be Expected from the GRACE-FO Laser Ranging Interferometer for Earth Science Applications? - *Surveys in Geophysics*,*37*, 2, pp. 453–470.

DOI: http://doi.org/10.1007/s10712-015-9338-y

What can be expected from the GRACE-FO Laser Ranging Interferometer for Earth Science applications?

Frank Flechtner[1*], Karl-Hans Neumayer[1], Christoph Dahle[1], Henryk Dobslaw[1], Elisa Fagiolini[1], Jean-Claude Raimondo[2], Andreas Güntner[3]
1: GFZ German Research Center for Geosciences, Department 1 “Geodesy and Remote Sensing”, Telegrafenberg, D-14473 Potsdam, Germany
2: SpaceTech GmbH, Seelbachstr. 13, D-88090 Immenstaad, Germany
3: GFZ German Research Center for Geosciences, Department 5 “Earth Surface Processes”, Telegrafenberg, D-14473 Potsdam, Germany

*: Corresponding author: Frank Flechtner (e-mail: frank.flechtner@gfz-potsdam.de, tel: 0049-331-288-1130, fax: 0049-331-288-1169)

Abstract

The primary objective of the Gravity Recovery and Climate Experiment follow-on (GRACE-FO) satellite mission, due for launch in August 2017, is to continue the GRACE time series of global monthly gravity field models. For this, evolved versions of the GRACE microwave instrument (MWI), GPS-receiver, and accelerometer will be used. A secondary objective is to demonstrate the effectiveness of a laser ranging interferometer (LRI) in improving the satellite-to-satellite tracking measurement performance. In order to investigate the expected enhancement for Earth science applications we have performed a full-scale simulation over the nominal mission lifetime of five years using a realistic orbit scenario and error assumptions both for instrument and background model errors.

Unfiltered differences between the synthetic input and the finally recovered time-variable monthly gravity models show notable improvements with the LRI, on global scale, of the order of 23%. The gain is realized for wavelengths smaller than 240 km in case of Gaussian filtering but decreases to just a few percent when anisotropic filtering is applied. This is also confirmed for some typical regional Earth science applications which show randomly distributed patterns of small improvements but also degradations when using DDK4 filtered LRI based models.

Analysis of applied error models indicates that accelerometer noise followed by ocean tide and non-tidal mass variation errors are the main contributors to the overall GRACE-FO gravity model error. Improvements in these fields are therefore necessary, besides optimized constellations, to make use of the increased LRI accuracy and to significantly improve gravity field models from Next Generation Gravity Missions.

Keywords: GRACE; GRACE-FO; time variable gravity modeling; satellite-to-satellite tracking

1. Introduction

The GRACE (Gravity Recovery and Climate Experiment) mission (Tapley et al. 2004) launched in 2002 is the only mission capable to monitor mass variations in the Earth system. Major advances that GRACE has provided in Earth sciences have recently been summarized by Wouters et al. (2014). Prominent examples are:

- Mass balancing of the continental water content, which is ultimately a sum of precipitation, evaporation, runoff and storage, enabling us to monitor the season-dependent changes in the major river basins, as well as huge groundwater extraction due to irrigation e.g. in India (Rodell et al. 2009) or California (Scanlon et al. 2012).
- Quantification of the increase or decrease of the ice and snow masses in the polar or large glacier areas has been achieved by scientists who were able to demonstrate a strong correlation between the climatic phenomenon ENSO / La Nina, the rainfall patterns in West Antarctica and the reduction of ice mass there (Sasgen et al. 2010).
- Monitoring of global mean eustatic sea-level variations as a consequence of mass re-distribution between continents and ocean basins for the partitioning of observed sea-level changes into mass and temperature contributions (Cazenave et al. 2009), as well as the regional re-distribution of water masses in response to time-variable surface winds that are tightly connected to time-variations of hemispheric current systems such as the Antarctic Circumpolar Current (Bergmann and Dobslaw (2012)).
- Observation of changes in the solid Earth following large earthquakes, such as Sumatra-Andaman (2004), Chile (2010) and Fukushima (2011, Wang et al. 2012).

These results are based on the more than 13-years-long time series of monthly estimates of the global gravity field of the Earth. All GRACE instruments are still producing nominal high quality observation data, the solar activity is still moderate, and fuel consumption is still lower than predicted. Therefore, the mission lifetime of GRACE could in principle be extended through 2018. Unfortunately, the batteries on both satellites are degrading and as a consequence the accelerometer (to observe non-gravitational forces due to atmospheric drag or solar radiation pressure), the Instrument Control Units, and/or the Microwave Assembly (part of the microwave instrument (MWI) K-band inter-satellite ranging system) are powered off during the maximum eclipse season, thus interrupting the nominal science data flow every 161 days for a period of approximately 3-4 weeks (Flechtner et al. 2015). Further information on the mission status is regularly provided at http://www.csr.utexas.edu/grace/operations/mission_status.

Due to the tremendous success of GRACE data applied in many Earth science disciplines there has been a long standing strong request by the international user community to launch a GRACE Follow-On (GRACE-FO) mission as fast as possible to extend the mass flux time series with the minimum practical data gap between both missions. GRACE-FO is, as GRACE, again implemented under US-German partnership (Flechtner et al., 2015). Overall mission management and satellite and instrument responsibility is with the Jet Propulsion Laboratory (JPL) which will procure the satellite buses and accelerometers, provide the microwave instrument, GPS receiver, and a significant portion (electronics, laser) of a joint Laser Ranging Interferometer (LRI). Germany will provide the launch vehicle, perform mission operations, participate in the joint Science Data System (SDS) and will provide major (optical) contributions to the LRI. All German contributions are managed by the GFZ German Research Centre for Geosciences. The NASA/GFZ partnership is stipulated in a Memorandum of Understanding (MOU), the roles and responsibilities in a Cooperative Project Plan (CPP). GRACE-FO passed the Preliminary Design Review (PDR) in January 2014 and entered Phase-C in March 2014. The Critical Design Review (CDR) was successfully completed in February 2015. The System Integration Readiness Review (SIR) was successfully performed in July 2015. Both satellites shall be launched with a Russian DNEPR in August 2017 into a circular polar orbit with an initial altitude of 490 km.

The primary objective of the GRACE-FO mission is to continue the record of climate change observations established by GRACE by extending the time series of high-resolution monthly global models of the Earth's gravity field for an additional five years period (Flechtner et al. 2015). For this, evolved versions of the GRACE microwave instrument (MWI), GPS-receiver, and accelerometer will be used. Whenever possible, lessons learnt from GRACE will be taken into account to improve the GRACE-FO MWI based gravity field models. For example, GRACE-FO attitude control will be based on three star camera heads instead of two in the case of GRACE. This will make attitude determination more robust (especially in phases of blinding by the Sun and/or the Moon). Also the radiator on the bottom of the GRACE-FO spacecraft will be rigid instead of using foils on GRACE to get rid of artificial signals (so called "twangs") observed in the GRACE accelerometer records (Flury et al. 2008). A secondary GRACE-FO objective is to demonstrate the effectiveness of the LRI in improving low-low satellite-to-satellite (SST) measurement performance which is directly linked to the accuracy of the derived gravity field models (Sheard et al. 2012). The LRI will be the first ever inter-spacecraft laser interferometer and should lead to improved spatial and temporal resolution for future Next Generation Gravity Missions (NGGM). Another secondary objective is to continue GRACE radio occultation measurements for operational provision of temperature or humidity profiles of the neutral atmosphere to numerical weather services (Wickert et al. 2009).

In a previous study, Loomis et al. (2012) investigated the accuracy and spatial resolution of monthly gravity field recovery using several possible configurations of a GRACE-FO mission by a simulation experiment covering a 25 months period. These scenarios were based on a GRACE-like orbit at 480 km altitude and 220 km separation using on-board accelerometers with the same noise characteristic as GRACE, and alternatively flying in drag-free mode at 250 km altitude at 50 km separation. They investigated the ability of these configurations to recover 1° x 1° mascon blocks in Greenland and in the Amazon basin in presence of instrument and background model errors. The MWI SST range-rate errors were assumed as for GRACE (0.2 μm/s) and for the Laser SST measurement performance they assumed an optimistic (laboratory) value of 0.6 nm/s. Their main conclusion was that the increased precision of the laser link does not improve gravity estimation when flown with GRACE-like on-board accelerometers, altitude and spacecraft separation and that also only modest improvement is realized for the best case scenario (laser, low-altitude, drag-free) primarily due to temporal aliasing errors.

As the GRACE and GRACE-FO Science Data Centers (UTCSR, JPL and GFZ) will base their monthly Level-2 gravity field model estimates on spherical harmonics we have performed a new full-scale simulation over the nominal five years mission period we have performed a new full-scale simulation over the nominal five years mission period in order to investigate possible improvements by the LRI on GRACE-FO when compared to GRACE-FO MWI derived gravity models. The intention of the paper is not to compare the gain of GRACE-FO with respect to GRACE when analyzing baseline MWI data. In contrast to Loomis et al. (2012) we did not just use the difference of two atmosphere and ocean models to take into account high-frequency aliasing errors, but applied a reasonably perturbed background model of non-tidal atmosphere and ocean variability that is part of the updated ESA Earth System Model specifically prepared for future gravity mission simulations (Dobslaw et al., 2015a, 2015b).. Finally, the Loomis et al. (2012) assumptions for LRI instrument noise were updated according to the actual GRACE-FO specifications (Sheard et al 2012). The orbital decay, ground track pattern and orbital errors were simulated in order to fit to the real GRACE and expected GRACE-FO situation. In contrast to the mascon results, the GRACE spherical harmonic solutions require post-processing (filtering) in order to get rid of artificial striping due to increasing spherical harmonic errors with increasing degree and for specific orders. For this we applied and compared different isotropic and anisotropic filters with various resolutions such as Gaussian averaging (Wahr et al. 1998), the so-called DDK filtering (Kusche 2007) or the destriping method by Swenson and Wahr (2006).

Our simulation assumptions and strategy are explained in Sect. 2. The global results, when comparing the recovered GRACE-FO MWI and LRI monthly gravity model time series with the simulated “true world” input gravity signals are then described in the spectral and spatial domain (Sect. 3). Section 4 focuses on typical GRACE-FO regional results for hydrological, glaciological, oceanographic or solid Earth applications. In Section 5 we investigate the various contributions of instrument and background model errors to the overall MWI and LRI based result. A summary and our conclusions are provided in Sect. 6.

2. Simulation Assumptions and Strategy

The five years full scale simulation is based on realistic assumptions for the upcoming GRACE-FO mission. The simulated orbits start at the target initial altitude of 490 km with an inclination of 89.0° and an eccentricity of 0.0015 and end at an altitude of about 450 km after the nominal GRACE-FO mission lifetime of 5 years. This decay of about 40 km is similar to the early GRACE mission descent. The solar activity values (necessary to simulate non-gravitational forces and accelerometer data, respectively) were taken from the period 1995-1999 which should represent similar characteristics as expected for 2018-2022. In order to maintain the inter-satellite link between 170 and 270 km it was necessary to apply a reset of the inter-satellite distance each year (the same is done by regular orbit maintenance maneuvers during the GRACE mission lifetime). The simulated osculating altitude, satellite separation and solar activity values are shown in Fig. 1. We have not simulated any orbit maneuver to keep the ground track spacing dense throughout the complete mission period. Such kind of maneuvers are also not performed within the GRACE mission and led to temporary unfavorable repeat cycles (see http://www.gfz-potsdam.de/grace) e.g. in September 2004 (4 days) or February 2015 (2 days). Fig. 2 depicts the ground track patterns for August 2019 (worst case within the five years, see Fig. 3), March 2021 (not optimal, but sufficient enough for nominal gravity field recovery) and May 2021 (representative month for an optimal sampling scenario).

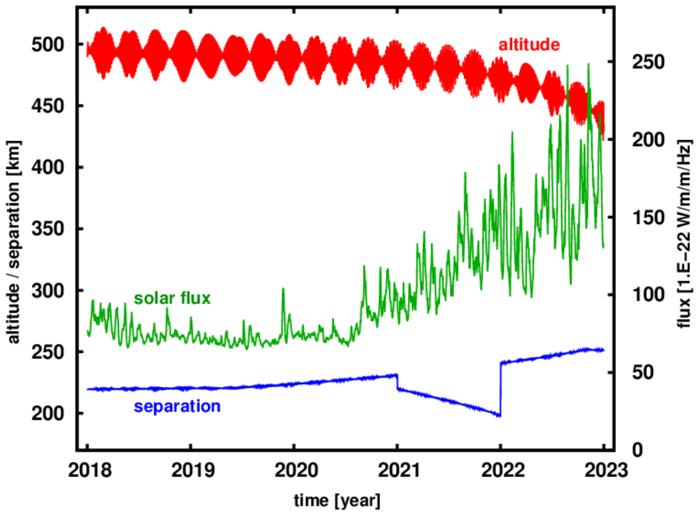

Fig. 1 Simulated osculating altitude, minimum and maximum satellite separation and solar flux values

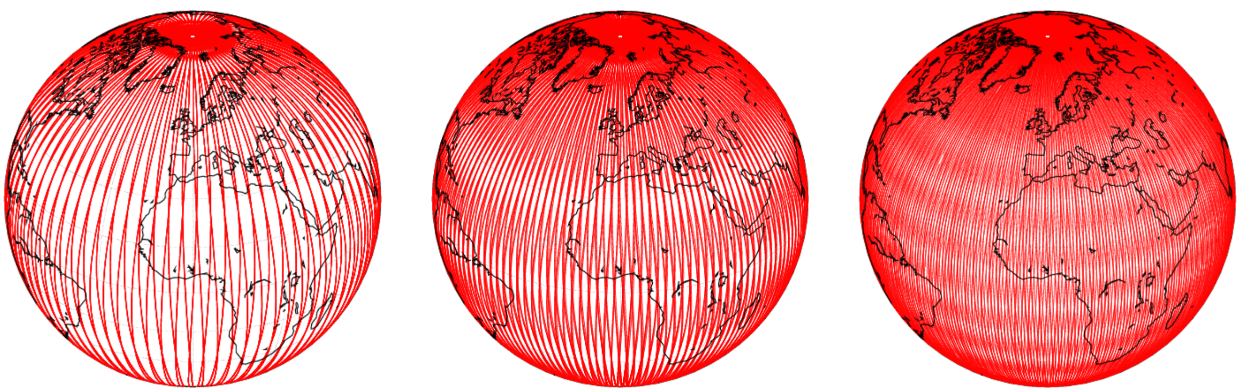

Fig. 2 Ground track pattern for August 2019 (left), March 2021 (middle) and May 2021 (right)

In a first (forward simulation) step, 5-seconds (integration step size as for GRACE) satellite orbits and true SST observations have been simulated using GFZ´s Earth Parameter and Orbit System (EPOS) software package which is also operationally applied for GRACE real data analysis. Non-gravitational forces have been simulated from models for atmospheric drag (MSIS86, Hedin 1987), solar radiation pressure (umbra and penumbra using solar flux values as depicted in Fig. 1), and Earth albedo and infrared (Knocke et al. 1988). The sum of these accelerations has been converted into pseudo GRACE-FO 3D accelerometer data. For nominal attitude we assumed yaw steering. Additional background models applied during simulation included a static gravity model (EIGEN-GL04C (Förste et al. 2008, used up to degree and order 100), Sun and Moon ephemerides (DE405, Standish 1998), ocean tides (the 8 main constituents Q1, O1, P1, K1, N2, M2, S2 and K2 of EOT08a, Savcenko et al. 2008), and non-tidal mass variations in atmosphere, oceans, hydrology, ice, and solid Earth (called AOHIS in the following) from the updated ESA Earth System Model (Dobslaw et al. 2015a, used up to degree and order 100). The high-low SST GPS phase and code observations, used to define a reference frame for LEO orbit integration (Reigber et al. 2005) have been simulated with white noise of 0.3 and 30 cm, respectively.

In the next step we have added colored noise to the simulated MWI, LRI and accelerometer data. As no realistic star camera attitude noise was available for the authors of this study (and has, likely for the same reasons, also not been treated in other GRACE-FO simulations, e.g. Loomis et al. 2012) we have referred both the simulated MWI and LRI observations to the center of mass (CoM) of the GRACE-FO spacecraft and have neglected any attitude error impact, especially on the SST data. The MWI is located about 1.4 m off from the CoM while the LRI is virtually measuring to the CoM, thanks to its racetrack design and the Triple Mirror Assembly (Sheard et al. 2012). Consequently, attitude errors would primarily impact the MWI-based results. Bandikova and Flury (2014) have analyzed GRACE

Level-1B star camera data and reported systematically higher noise than expected. The reason was found in the incorrect implementation of algorithms for quaternion combination in the JPL processing routines. Bandikova et al. (2014) investigated the impact on gravity field determination and found that neither the Celestial Mechanics Approach nor the Variational Equations Approach is sensitive to these noise errors. Therefore, attitude errors have not been treated in our study.

The 5 second SST noise values for MWI and LRI are modeled in terms of amplitude spectral density (ASD) as a square root of power spectrum density (PSD) with a distance-dependent factor for which we applied the average distance between the two GRACE-FO satellites (220 km). The method is described in Elsaka et al. (2014) and the values applied in our study are consistent with the expected performance of the GRACE-FO LRI (Sheard et al. 2012) and MWI (Dahle et al. 2014) SST noise: LRI 80 nm (range) resp. 9.9 nm/s (range-rate); MWI: 2.1 µm (range) resp. 0.24 µm/s (range-rate). The LRI instrument has lower errors in the high frequency part of the spectrum (Sheard et al. 2012) which ultimately could result in improved estimation of GRACE-FO high-degree spherical harmonic coefficients (as shown in the simulation results in Figure 10). Also, it has to be mentioned that, as for GRACE GFZ real data analysis, the MWI and LRI based simulations are made with range-rate SST data only. The procedure to derive accelerometer noise time series using spectral density values for a frequency (f) band of 10^{-4} to 10^{-1} Hz of GRACE-like accelerometer errors ($(1 + 0.005/ f)^{1/2} \times 10^{-10}$ m/s^2/Hz$^{1/2}$ for transversal and radial direction, $(1 + 0.1/ f)^{1/2} \times 10^{-9}$ m/s^2/Hz$^{1/2}$ for normal direction) was the same as described in Loomis et al. (2012).

In the backward simulation performed again with EPOS software, we used the simulated observations, supplemented with the colored MWI, LRI and ACC noise, to recover the 60 monthly gravity field models up to degree and order 100. Here we also substituted the nominal background models to simulate a realistic error level in the static and time variable gravity field. For this we used EGM96 (Lemoine et al. 1998) up to degree and order 100 as static gravity model and substituted the 8 main ocean tide constituents by GOT4.7 (Ray 2008) values.

As the a priori background model for the non-tidal mass variability in atmosphere and oceans, we employed the realistically perturbed de-aliasing model Dobslaw et al. (2015b) which is part of the updated ESA Earth System Model. This perturbed background model contains (i) errors at large spatial scales that have been derived from appropriately scaled differences with the original ESA Earth System Model (Gruber et al., 2011) assessed individually for periods between 10 - 30, 3 - 10, and 1 - 3 days, the S1 atmospheric tide, and sub-diurnal periods. Further, the model includes (ii) errors at small spatial scales typically not covered by global models of atmosphere and ocean variability; and finally (iii) errors due to physical processes not represented in currently available de-aliasing products as GRACE AOD1B (Flechtner et al. 2014). The updated ESA Earth System Model including the perturbed background model is publicly available together with its technical documentation via doi 10.5880/GFZ.1.3.2014.001.

The gravity recovery step was performed twice: in a first run we used explicitly the MWI data and in the second run we applied only the LRI data. All other observations (accelerometer, GPS) and background model errors were identical in both cases as this would also be the case during GRACE-FO real data analysis. Besides spherical harmonic coefficients also arc-specific parameters such as initial orbital states and 3-hourly 3D accelerometer biases and scales have been adjusted (similar to GRACE RL05a). The resulting MWI and LRI based monthly gravity solutions have then been compared with the simulated ("true") gravity field time series in the spectral and spatial domain as well (if applicable) with real GRACE results to show that the simulated gravity results are as realistic as possible. For example, to check the simulated orbit accuracy we have analyzed the satellites separation derived from GPS data only. For this we have intentionally down-weighted the MWI data (which have usually a very high weight in order to derive mid to short wavelength gravity coefficients). The resulting global GPS-derived range-rate residual root mean square (RMS) values can then be interpreted as a measure of the orbit accuracy by comparing them with the much more precise MWI observations serving as a reference. The results were typically in the order of 1.5 µm/s which is identical to GFZ GRACE RL05 real data analysis (e.g. for June 2014).

3. Results in the spectral and spatial domain

As a measure of the true error of our simulated gravity field models, unfiltered monthly differences between the recovered and the a-priori static gravity field model plus the monthly mean HIS component of the time-variable AOHIS a priori model are used. Fig. 3 shows these errors in terms of latitude weighted RMS (wRMS) of equivalent water heights (EWH) for the complete simulation period of five years (2018-2022). The two curves depict the result obtained using the baseline MWI SST and the demonstrator LRI observations. It becomes visible that for the unfiltered case the LRI outperforms the MWI derived results for all months. The two peaks in August 2019 and November 2021 are correlated with imperfect ground track coverage compared to other months (see Fig. 2 left).

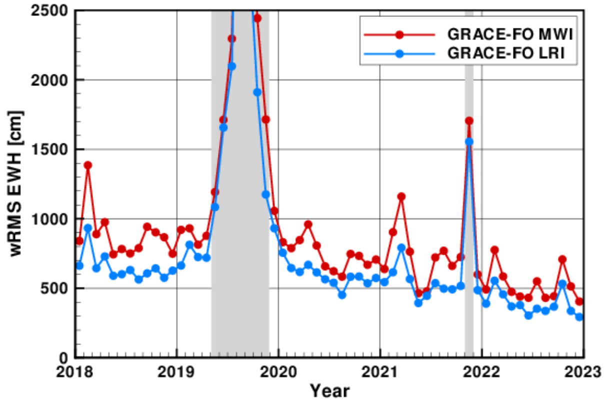

Fig. 3 Unfiltered monthly differences between recovered and simulated gravity fields in terms of the weighted root mean square (wRMS) of equivalent water heights (EWH) for the five years simulation period using simulated GRACE-FO MWI (red) and LRI (blue) data. Periods with imperfect ground track pattern have been marked grey

Table 2 shows the corresponding mean wRMS values of 52 (neglecting the grey periods highlighted in Fig. 3) monthly MWI and LRI based models in terms of EWH for the unfiltered case and after application of various filters. Filtering is necessary to reduce degree-dependent errors for mid-to-long wavelengths resulting in a decrease of the EWH error from meter to centimeter level. It is clear that, for the unfiltered case on a global scale and on average the LRI observations will outperform the MWI results by 23 % in terms of wRMS reduction. The corresponding gain for the anisotropic DDK filtered global results is much smaller (about 1-7 %), whereas in case of applying destriping and/or Gaussian smoothing the gain by LRI becomes again more significant (about 15-23 % depending on the Gaussian filter radius). As the Gaussian filter removes high-frequency signals this filter is not used for regional analysis in Sect. 4. Note that typical GRACE RL05 GFZ (degree 90) and CSR (degree 96) monthly models show comparable unfiltered values, proving again that our results are realistic.

Table 2 Mean of monthly MWI- and LRI-based wRMS results in terms of EWH for the unfiltered case and after application of various filters. Note that 8 months with exceptionally large wRMS values due to repeat orbit pattern (marked with grey background color in Fig. 3) have been omitted.

Filter	MWI mean wRMS [cm]	LRI mean wRMS [cm]	mean wRMS reduction [%]
Unfiltered	736.64	564.56	22.9
DDK1 (530 km)	0.70	0.68	1.7
DDK2 (340 km)	1.20	1.19	1.0
DDK3 (240 km)	2.29	2.25	1.7
DDK4 (220 km)	2.73	2.66	2.6
DDK5 (160 km)	4.25	3.97	6.5
Destriping & Gauss 530 km	0.70	0.69	1.2
Destriping & Gauss 340 km	0.94	0.91	3.1
Destriping & Gauss 240 km	3.01	2.64	12.6
Destriping & Gauss 220 km	4.64	3.96	15.1
Destriping & Gauss 160 km	17.59	13.67	23.6
Gauss 530 km	1.13	1.15	-1.5
Gauss 340 km	2.95	2.79	4.7
Gauss 240 km	16.23	13.65	15.1
Gauss 220 km	26.31	21.67	16.8
Gauss 160 km	110.62	87.23	20.4

Fig. 4 shows unfiltered error degree amplitudes in terms of EWH for March 2021 and May 2021. March 2021 is chosen (also for the following figures) because it represents a non-optimal, but still sufficiently dense ground track pattern for nominal gravity field recovery and May 2021 is a representative month for an optimal sampling scenario (see Fig. 2). It becomes obvious that in the first case (March 2021) the LRI slightly improves the MWI errors in the mid (below degree 40 (500km)) and notable in the short wavelengths above degree 60 (333 km) while in the second case no improvement is seen by the LRI.

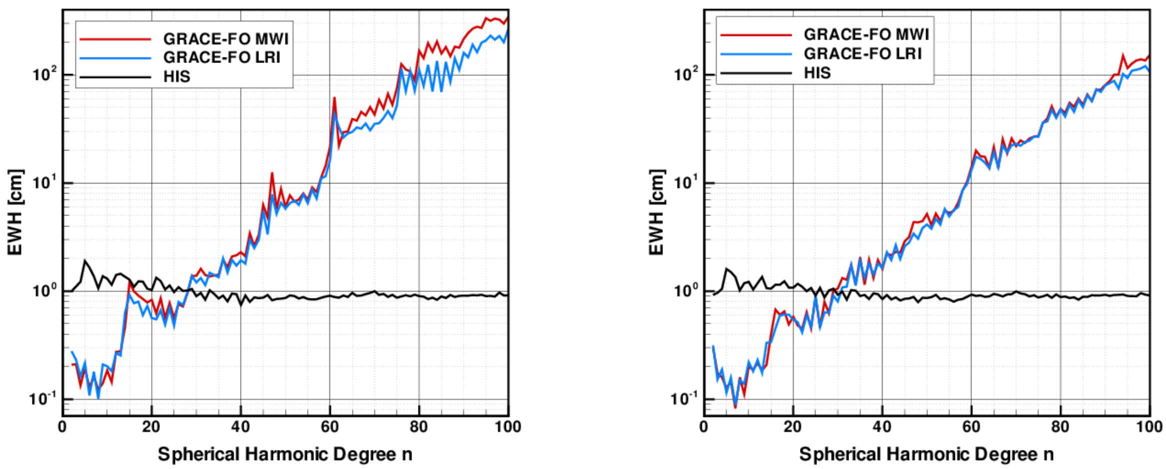

Fig. 4 Simulated MWI (red) and LRI (blue) difference degree amplitudes with respect to the “truth” in terms of EWH for March 2021 (left) and May 2021 (right). The true signal is given by the monthly mean of the HIS component of the AOHIS background model (black)

Similar conclusions can be drawn when looking at the cumulative difference degree amplitudes for the two test months (Fig. 5). While for an optimal sampling the LRI does not improve the gravity recovery error for all wavelengths (May 2021), the March 2021 scenario with non-optimal ground track pattern shows moderate improvements by the LRI for all wavelengths above 1000 km, e.g. the error will reduce from 4 to 3 cm EWH (600 km resolution) and from 20 to 15 cm EWH (400 km), respectively.

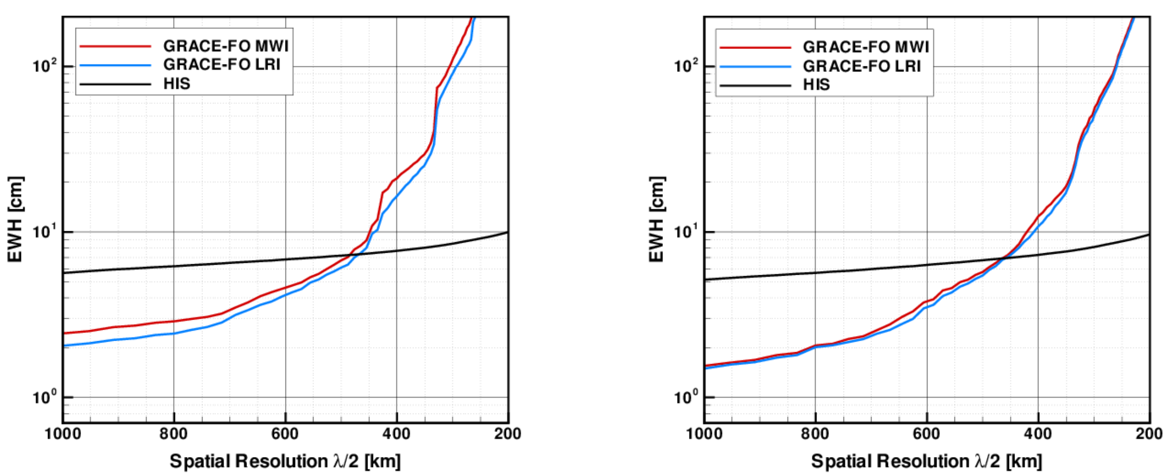

Fig. 5 Simulated MWI (red) and LRI (blue) cumulative difference degree amplitudes with respect to the “truth” in terms of EWH for March 2021 (left) and May 2021 (right). The true signal is given by the monthly mean of the hydrology, ice and solid Earth (HIS) component of the AOHIS background model (black)

Another way to visualize the results is shown in Fig. 6 where the unfiltered true and formal errors per degree and order for May 2021are shown in a logarithmic scale. The formal errors are those from adjustment procedure while the true errors are those described above. For comparison, GRACE real data errors based on the GFZ RL05a solution for May 2005 are shown as well. For the latter, the true error has been approximated by taking the difference between the solution and its static background model (EIGEN-6C, Shako et al. 2014) plus the time-variable part of EIGEN-6C (up to degree and order 50). The GRACE real and simulated MWI data show very similar error behavior, thereby verifying that the simulations have been done realistically. In contrast, the near zonal coefficients for spherical harmonic degrees above 60 are much better determined when simulated LRI observations are used. This confirms the improvements by LRI in the short wavelengths (Fig. 4).

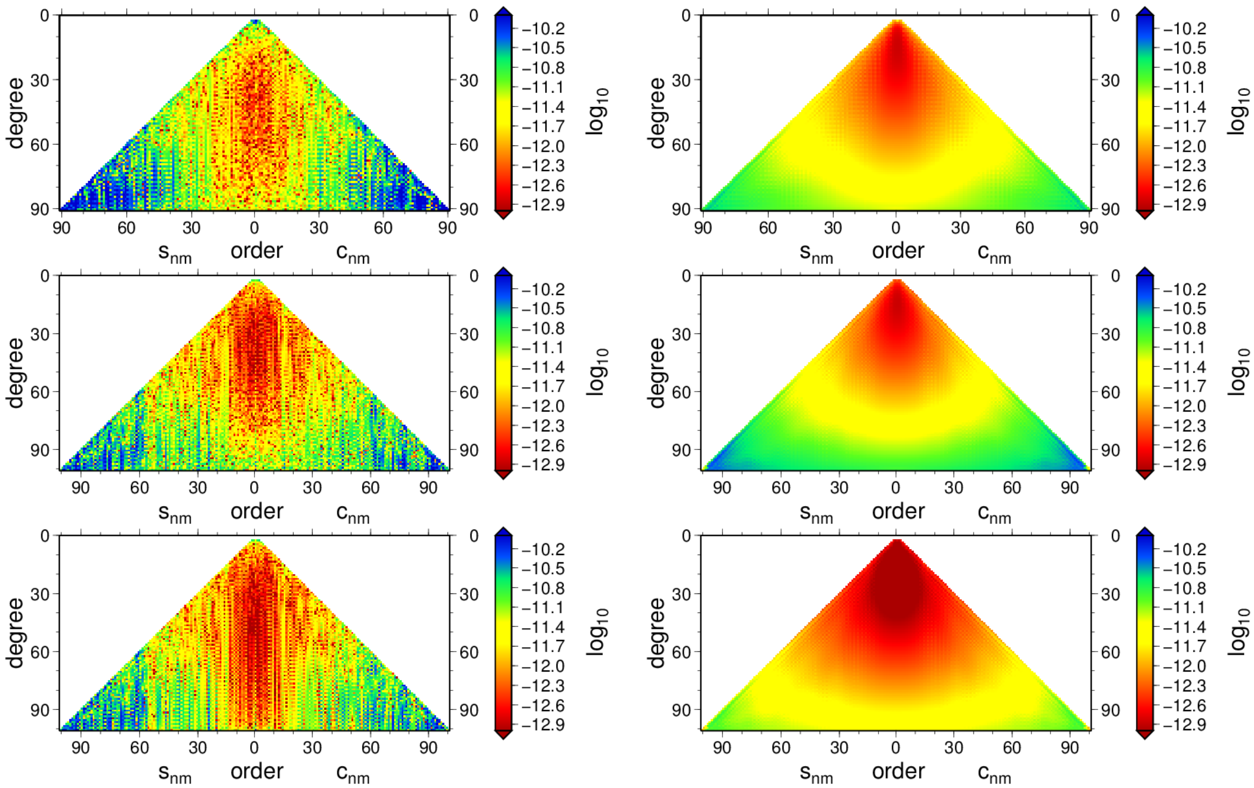

Fig. 6 GRACE real data (top), simulated GRACE-FO MWI (middle) and LRI (bottom) true (left) and formal (right) errors per degree and order for May 2005 (real data) and May 2021, respectively. Note that the maximum degree and order is l00 for the simulated GRACE-FO cases whereas it is limited to 90 for GRACE real data

Fig. 7 depicts the March and May 2021 unfiltered errors in the spatial domain in terms of geoid height errors. It becomes obvious that the error pattern of both months differ consistently with the ground track pattern shown in Fig. 2. In the case of a non-optimal sampling period (March 2021) the artificial spurious North-South stripes due to instrument or aliasing errors are significantly reduced by approximately 30% when substituting MWI by LRI SST observations. In case of an optimal sampling (May 2021) the MWI errors are reduced by only about 15%. The different contributions of instrument and background model errors to the total result are discussed in Sect.5.

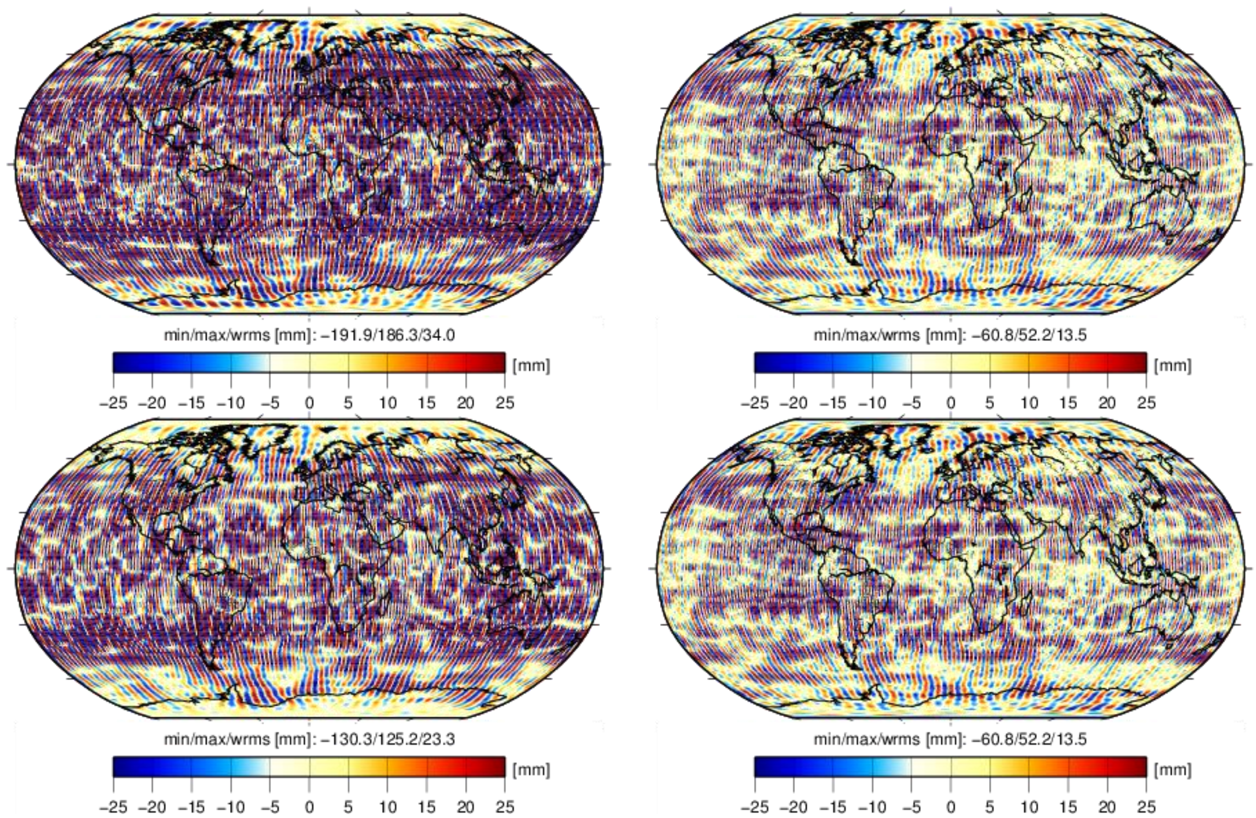

Fig. 7 Spatial difference between simulated ("true") and recovered gravity fields in terms of unfiltered geoid heights for March 2021 (left) and May 2021 (right) for the MWI (top) and LRI (bottom) based results

4. Regional applications using simulated MWI and LRI Data

It has been demonstrated in the previous section that the LRI will improve the MWI based unfiltered and filtered gravity models on a global scale only moderately and only in case of a non-optimal ground track pattern. As these globally averaged results are not meaningful for Earth system applications which have mass variation signals in defined areas such as changes in hydrological basins or melting of glaciers we have also investigated how seasonal, sub-seasonal, trend and instantaneous (Earthquake) signals as included in the AOHIS source model are recovered when using GRACE-FO MWI or LRI data.

Fig.8 left shows the RMS variability over 5 years (52 models of table 2) of the difference between simulated ("true") and DDK4 filtered recovered gravity fields based on LRI data in terms of EWH for 1° regular grids. The corresponding plot for MWI based gravity fields is quite similar and thus is not shown. Generally, the largest error variability (up to 150 cm EWH) is visible where ice or solid Earth signals are introduced by the AOHIS model. The difference between the RMS variability for MWI and LRI is shown in Fig. 8 right (red means LRI is closer to the truth and blue means MWI is closer to truth) and confirms that only moderate improvements up to 13 cm EWH can be expected from LRI data; however, also degradations up to 2 cm become visible.

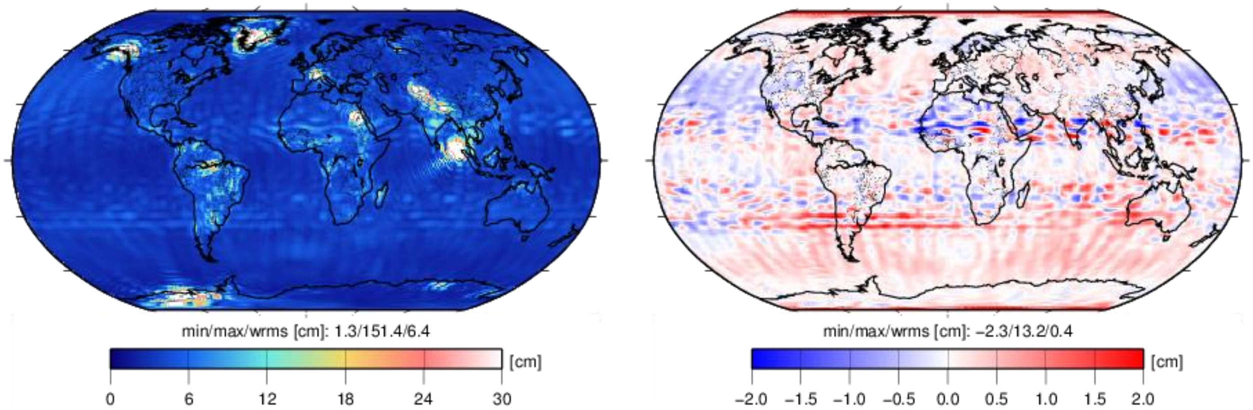

Fig. 8 RMS variability of difference between simulated ("true") and DDK4 filtered recovered gravity fields based on LRI over the 5 years investigated in terms of EWH (left). The difference between the RMS variability for MWI and LRI is shown in the right figure (red means LRI is closer to truth, blue means MWI is closer to truth)

Fig. 9 shows the DDK4 filtered time series in EWH for various 2ºx2º grid boxes such as the Amazon and the Danube river basins, the Greenland and West-Antarctica ice sheet, the Bellingshausen basin in the Antarctic Circumpolar Current and the simulated Sumatra Earthquake in comparison to the corresponding components of the time variable source model AOHIS.

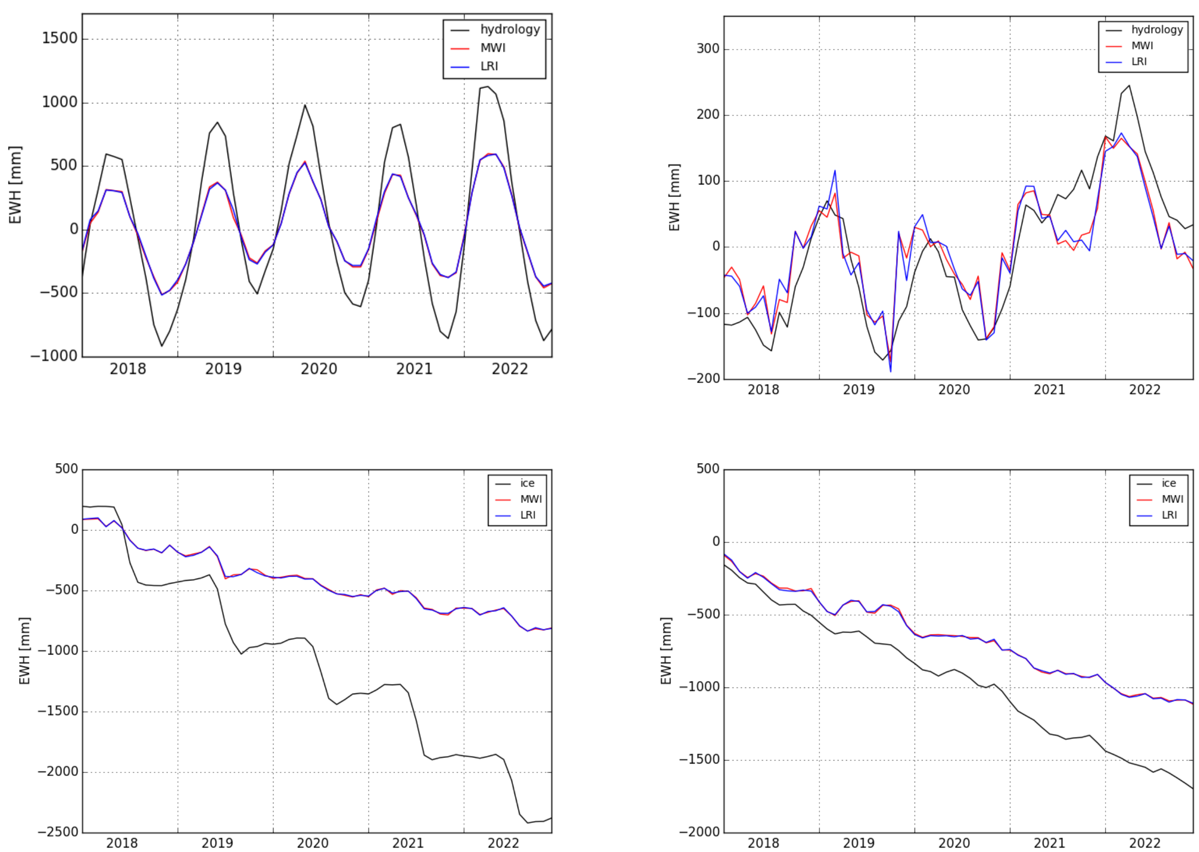

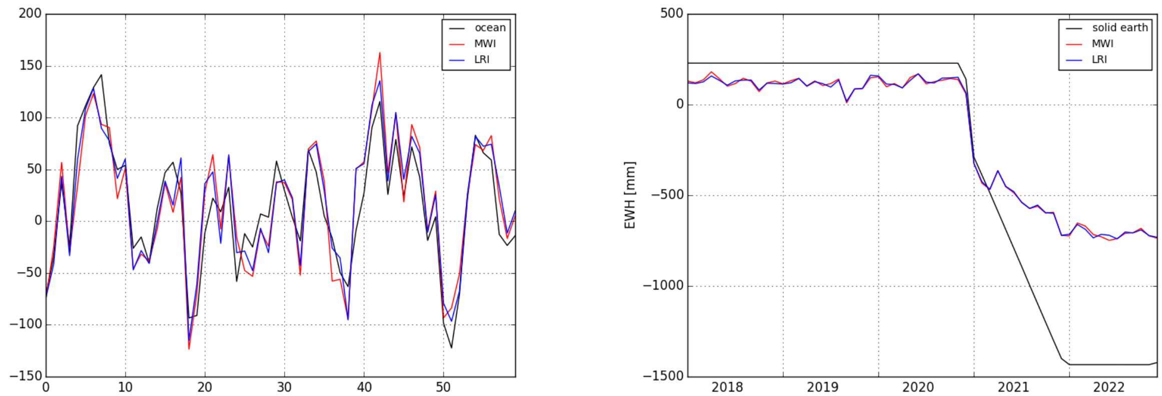

Fig. 9 Time series for DDK4 filtered 2ºx2º grid boxes in EWH [mm] for Amazon (top left) and Danube (top right), Greenland (middle left) and West-Antarctica (middle right) and Bellingshausen (bottom left) and for the simulated December 2004 Sumatra earthquake (now in December 2019, bottom right) using MWI (red) or LRI (blue) data. The black line depicts the corresponding component H, I, O and S of the AOHIS model

Table 3 summarizes these moderate improvements of the order of 2-15% in terms of error reduction when using LRI instead of MWI observations but also shows degradations for Amazon and Sahara (not shown in Fig 9).

To demonstrate how realistically our simulation was performed we have derived monthly DDK4 filtered differences between CSR RL05 and GFZ RL05a Level-2 products, both after substitution of C20 by the suggested GRACE TN07 values, for the 5-year period from 2006 to 2010 as a measure for present-day GRACE uncertainties. As can be deduced from Table 3 the average factor w.r.t. the simulated MWI result is, neglecting the Amazon basin, of the order of 0.86. The reasons for this are many and could include either too optimistically (or neglected, see conclusion section) simulated errors or not-investigated leakage effects in the simulation.

Table 3 RMS between recovered and simulated AOHIS signals [mm EWH] for various 2ºx2º grid boxes after DDK4 filtering as well as corresponding LRI gain [%] in terms of RMS reduction. Additionally, the DDK4 filtered "real data errors" [mm] derived from CSR and GFZ GRACE RL05 Level-2 data and the corresponding factor w.r.t. the simulated MWI RMS values are shown.

	MWI RMS [mm]	**LRI RMS [mm]**	**LRI Gain [%]**	**RL05 CSR-GFZ RMS [mm]**	**Factor RL05 / MWI**
Sumatra	33,58	31,52	6,5	30,57	0,91
Bellingshausen	26,44	22,93	15,3	21,83	0,83
Amazon	23,95	25,49	-6,0	42,88	1,79
Danube	31,78	32,17	-1,2	27,93	0,88
West Antarctica	25,60	25,18	1,7	23,70	0,93
Greenland	29,94	28,50	5,1	21,12	0,71
Sahara	37,13	39,65	-6,3	32,30	0,87

5. Error Analysis

In order to find out which of the applied instrument and background model errors are the main contributors to the overall MWI and LRI derived global gravity model error (see section 3) we have investigated the influence of the single error components (instrument noise, static gravity field error, ocean tide error, and atmosphere and ocean (AO) de-aliasing error) on the solution for May 2021. In order to quantify a specific individual error contribution, the complete backward simulation step has been repeated with that specific error source omitted, and then the difference of that solution from the solution containing all error sources has been evaluated. Thus, the orbits are recomputed for each individual error source and not only the error propagation through the observations but also through the computed orbits is taken into account. Figure 10 shows the corresponding individual degree amplitudes in terms of geoid height error. It can be clearly seen that the impact of SST noise on gravity field recovery is significantly reduced if LRI instead of MWI observations are used. The spatial resolution where the signal-to-noise ratio equals one increases from degree 60 (333 km) to degree 80 (250 km). However, it becomes also obvious that the main contributors to still existing striping (see Fig. 7 right) are the accelerometer (ACC), ocean tide (otid) and AO errors. All other errors, including the MWI and LRI SST errors, are about one order of magnitude smaller. This confirms that, on a global scale, the decreased LRI noise cannot improve the monthly gravity model for a GRACE-like constellation. Consequently, Next Generation Gravity Missions (NGGM) which may consist of double GRACE-like pairs in a so called "Bender-constellation" and which will move along much lower orbits (Elsaka et al. 2014) have to significantly reduce these errors in order to benefit from improved LRI SST measurements.

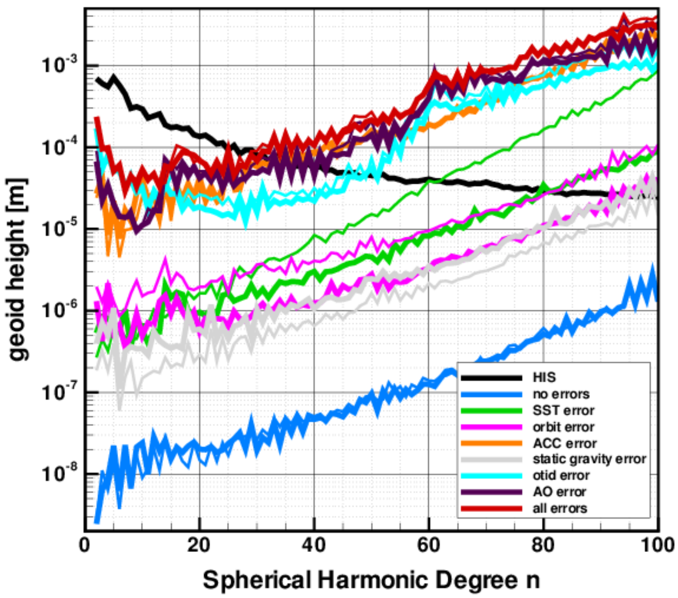

Fig. 10 Degree amplitudes in terms of geoid height error for May 2021 for different individual instrument and model errors (see legend). The thin and bold lines show the results obtained with MWI and LRI, respectively. The blue curve shows the numerical accuracy of the full scale simulations (no errors applied) which is about 3 orders of magnitude below the current GRACE-FO error level. The black line depicts the monthly mean HIS signal

Fig. 11 depicts the resulting spatial pattern for the three main error contributors. The corresponding RSS (root squared sum) gives 14.8 (MWI) and 11.8 (LRI) mm geoid height error which is consistent with the overall error of 13.5 (MWI) and 11.6 (LRI) mm of Fig. 7 right and proves that the other error sources, including SST noise, do not matter for a GRACE-like constellation.

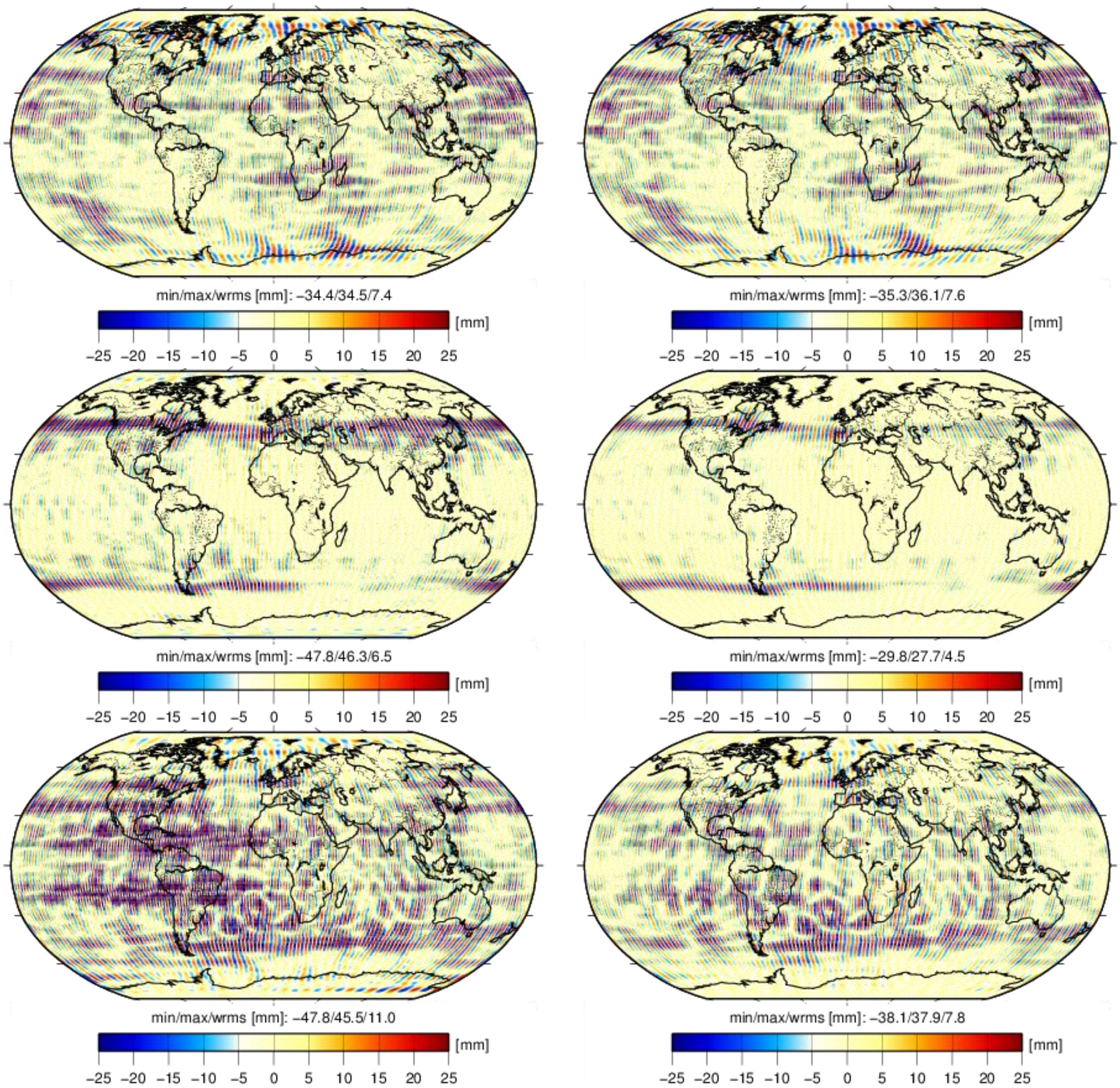

Fig. 11 Spatial difference between simulated ("true") and recovered gravity fields in terms of unfiltered geoid heights for MWI (left) and LRI (right) derived gravity models for May 2021 in case of ACC errors only (top), ocean tide errors only (middle) and AO errors only (bottom). Statistics show minimum, maximum and wRMS of errors

6. Summary and Conclusions

We have performed a full-scale simulation based on realistic assumptions for the GRACE-FO orbit scenario, instrument noise for accelerometer, MWI and LRI SST observations as well as background model errors for the static gravity field and tidal and non-tidal short-term mass variations to investigate the gain in monthly gravity field determination when using the LRI SST observations instead of MWI tracking data.

The results show that the 60 unfiltered LRI-derived monthly gravity field models always outperform the corresponding MWI-based results. The corresponding time series shows an approximately 23% smaller wRMS in terms of EWH when compared to the simulated "true world" scenario proving the expectations into the increased

LRI SST accuracy. The corresponding difference degree amplitudes and cumulative degree amplitudes for two test months March 2021 and May 2021 indicate that for non-optimal ground track pattern (March 2021) moderate improvements can be expected by the LRI for mid to short wavelengths. For that month also the near zonal coefficients for spherical harmonic degrees above 60 are much better determined when LRI observations are used. This is also visible in slightly less meridional striping in the spatial pattern. Applying isotropic Gaussian filtering in order to get rid of larger errors with increasing degree of spherical harmonic coefficients shows – on a global scale - also notable improvements of 13-23% at or below 240 km spatial resolution. In contrast, anisotropic filtering (DDK) results in only minor reduction (2-7%) of errors by the LRI instrument.

Looking into typical regional hydrological, glaciological, solid Earth and ocean applications in the Amazon or Danube basin, Greenland and West-Antarctica, the Sumatra Earth quake or the Bellingshausen basin in the Antarctic circumpolar current it can be concluded that the globally observed 2.6 % gain, when using DDK4 filtered LRI-derived monthly models, is not visible everywhere but shows a more or less randomly distributed pattern. There are regions like on the Southern oceans where we observe 15% smaller errors, but in the Amazon or Sahara we also simulated 6% larger errors when using LRI data.

The error assumptions for the accelerometer and SST data as well as for the non-tidal atmosphere and ocean mass variations have been made as realistic as possible. This is shown by comparison with real GRACE data such as GFZ RL05 orbit errors or remaining monthly gravity model errors as derived from comparison of CSR RL05 and GFZ RL05a solutions. Nevertheless, the ocean tide errors have been defined (due to lack of better knowledge) as the difference of two standard models which may not be fully realistic. Additionally, the gain which may be achieved using LRI data for GRACE-FO gravity field determination alone (neglecting the three main error contributors accelerometer noise and ocean tide and AOHIS background model errors) may be larger as we have not simulated attitude errors. This error would result in MWI phase center variations, but would not affect the LRI observations as they are already referred to the center of mass (using a triple mirror assembly, see Sheard et al. (2012)). Both, the ocean tide and attitude error are subjects for future investigations.

As a final conclusion it can be stated that the LRI will only moderately improve the MWI based GRACE-FO monthly gravity model time series. Earth Science applications will benefit much more from the continued time series based on GRACE data. The main expectation in the LRI is technology demonstration for future gravity missions. Here, full advantage will be gained when a LRI will be the prime instrument on a Next Generation Gravity Mission. This will probably be realized by the combination of a polar orbiting pair of satellites with a second pair of satellites in lower orbit and at smaller inclination, a LRI SST and improved accelerometers and attitude and orbit control system.

Acknowledgements.

The authors thank BMBF (German Ministry for Education and Research), BMWi (German Federal Ministry for Economics and Technology), HGF (German Helmholtz Foundation) and DLR (German Aerospace Center) for providing funding and in kind contribution for implementation of the German GRACE-FO mission elements.

The paper also arises from the ISSI (International Space Science Institute, Bern, Switzerland) Workshop on Remote Sensing and Water Resources in October 2014.

Compliance with Ethical Standards

The authors certify that they have NO affiliations with or involvement in any organization or entity with any financial interest (such as honoraria; educational grants; participation in speakers' bureaus; membership, employment, consultancies, stock ownership, or other equity interest; and expert testimony or patent-licensing arrangements), or non-financial interest (such as personal or professional relationships, affiliations, knowledge or beliefs) in the subject matter or materials discussed in this manuscript.

References

Bandikova T, Flury J (2014) Improvement of the GRACE star camera data based on the revision of the combination method, Advances in Space Research, 54:1818–1827, doi:10.1016/j.asr.2014.07.004

Bandikova T, Meyer U, Klinger B, Tregoning P, Flury J, Mayer-Gürr T (2014) Improved star camera attitude data and their effect on the gravity field. Proceedings of the GRACE Science Team Meeting (http://www.gfz-potsdam.de/en/section/globalgeomonitoringandgravityfield/topics/development-operation-and-analysis-of-gravity-field-satellite-missions/grace/gstm/gstm-2014/meeting-program-and-abstract-list/, last time visited August 4, 2015), German Research Centre for Geosciences, Potsdam, Germany, September 29-October 1, 2014.

Bergmann I, Dobslaw H (2012) Short-term transport variability of the Antarctic Circumpolar Current from satellite gravity observations. Journal of Geophysical Research (Oceans), 117(C16):5044. doi:10.1029/2012JC007872

Cazenave A, Dominh K, Guinehut S, Berthier E, Llovel W, Ramillien G, Ablain M, Larnicol G (2009) Sea level budget over 2003–2008: A reevaluation from GRACE space gravimetry, satellite altimetry and Argo. Global and Planetary Change, 65:83–88

Dahle C, Flechtner F, König R, Michalak G, Neumayer KH, Gruber C, König D (2014) GFZ RL05: An Improved Time-Series of Monthly GRACE Gravity Field Solutions, In: Flechtner, F., Sneeuw, N., Schuh, W.-D. (Eds.), Observation of the System Earth from Space - CHAMP, GRACE, GOCE and future missions, (GEOTECHNOLOGIEN Science Report; 20; Advanced Technologies in Earth Sciences), Berlin [u.a.] : Springer, p. 29-39. doi:1007/978-3-642-32135-1

Dobslaw H, Bergmann I, Dill R, Forootan E, Klemann V, Kusche J, Sasgen I (2015a) The updated ESA Earth System Model for future gravity mission simulation studies, Journal of Geodesy. doi:10.1007/s00190-014-0787-8

Dobslaw H, Bergmann-Wolf I, Forootan E, Dahle C, Mayer-Gürr T, Kusche J, Flechtner F (2015b) Modeling of present-day atmosphere and ocean non-tidal de-aliasing errors for future gravity mission simulations, submitted to Journal of Geodesy.

Elsaka B, Raimondo JC, Brieden P, Reubelt T, Kusche J, Flechtner F, Iran Pour S, Sneeuw N, Müller J (2014) Comparing seven candidate mission configurations for temporal gravity field retrieval through full-scale numerical simulation. Journal of Geodesy, 88:31–43. doi:10.1007/s00190-013-0665-9

Flechtner F, Dobslaw H, Fagiolini E (2014) AOD1B Product Description Document for Product Release 05 (Rev. 4.2, May 20, 2014), http://www.gfz-potsdam.de/en/aod1b

Flechtner F, Morton P, Watkins M, Webb F (2015) Status of the GRACE Follow-on Mission. Proceedings of the International Association of Geodesy Symposia Gravity, Geoid and Height System (2012, Venice, Italy), IAGS-D-12-00141

Flury J, Bettadpur S, Tapley, BD (2008) Precise accelerometry onboard the GRACE gravity field satellite mission, Advances in Space Research, 42:1414–1423, doi:10.1016/j.asr.2008.05.004

Förste C, Schmidt R, Stubenvoll R, Flechtner F, Meyer U, König R, Neumayer H, Biancale R, Lemoine J, Bruinsma S, Loyer S, Barthelmes F, Esselborn S (2008) The GeoForschungsZentrum Potsdam/Groupe de Recherche de Geodesie Spatiale satellite-only and combined gravity field models: EIGEN-GL04S1 and EIGENGL04C. Journal of Geodesy, 82 (2008), 331–346

Gruber Th, Bamber JL, Bierkens MFP, Dobslaw H, Murböck M, Thomas M, van Beek LPH, van Dam T, Vermeersen LLA, Visser PNAM (2011) Simulation of the time-variable gravity field by means of coupled geophysical models, Earth Syst. Sci. Data 3(1), 19-35, doi: 10.5194/essd-3-19-2011Hedin AE (1987) MSIS86 thermospheric model, Journal of Geophysical Research, 92. doi: 10.1029/JA092iA05p04649

Kusche J (2007) Approximate decorrelation and non-isotropic smoothing of time-variable GRACE-type gravity field models. Journal of Geodesy, 81:733–749. doi:10.1007/s00190-007-0143-3

Knocke P, Ries J, Tapley B (1988) Earth radiation pressure effects on satellites, Proceedings of the AIAA/AAS Astrodynamics Specialist Conference 1988, Washington DC, USA, 577–586. doi: 10.2514/6.1988-4292

Lemoine, FG, Kenyon SC, Factor JK, Trimmer RG, Pavlis NK, Chinn DS, Cox CM, Klosko SM, Luthcke SB, Torrence MH, Wang YM, Williamson RG, Pavlis EC, Rapp RH, Olson TR (1998) The development of the joint NASA GSFC and the National Imagery and Mappping Agency (NIMA) Geopotential Model EGM96. NASA/TP-1998-206861, 1998

Loomis BD, Nerem RS, Luthcke SB (2012) Simulation study of a follow-on gravity mission to GRACE. Journal of Geodesy, 86:319–335. doi:10.1007/s00190-011-0521-8

Ray R (2008) GOT4.7 (private communication). Extension of Ray R (1999) A global ocean tide model from Topex/Poseidon altimetry GOT99.2. NASA Tech Memo 209478, Sept. 1999

Reigber C, Schmidt R, Flechtner F, König R, Meyer U, Neumayer KH, Schwintzer P, Zhu SY (2005) An Earth gravity field model complete to degree and order 150 from GRACE: EIGEN-GRACE02S. Journal of Geodynamics, 39:1–10

Rodell M, Velicogna I, Famiglietti JS (2009) Satellite-based estimates of groundwater depletion in India. Nature, 460:999–1002. doi:10.1038/nature08238

Sasgen I, Dobslaw H, Martinec Z, Thomas M (2010) Satellite gravimetry observation of Antarctic snow accumulation related to ENSO. Earth and Planetary Science Letters, 299:352–358. doi:10.1016/j.epsl.2010.09.015

Savcenko R, Bosch W (2008) EOT08a – empirical ocean tide model from multi-mission satellite altimetry, Report No. 81, Deutsches Geodätisches Forschungsinstitut (DGFI), München, 2008

Scanlon BR, Longuevergne L, Long D (2012) Ground referencing GRACE satellite estimates of groundwater storage changes in the California Central Valley, USA. Water Resources Research, 48:4520. doi:10.1029/2011WR011312

Shako R, Förste C, Abrikosov O, Bruinsma SL, Marty JC, Lemoine JM, Flechtner F, Neumayer KH, Dahle C (2014) EIGEN-6C: A High-Resolution Global Gravity Combination Model Including GOCE Data. In: Flechtner F et al (eds) Observation of the System Earth from Space - CHAMP, GRACE, GOCE and Future Missions, Advanced Technologies in Earth Sciences. Springer, Berlin/Heidelberg. doi:10.1007/978-3-642-32135-1_20

Sheard B, Heinzel G, Danzmann K, Shaddock D, Klipstein B, Folkner W (2012) Intersatellite laser ranging instrument for the GRACE follow-on mission, Journal of Geodesy, 29. doi:10.1007/s00190-012-0566-3

Standish E (1998) JPL planetary and lunar ephemerides “DE405/LE405”. Interoffice Memorandum IOM 312.F-98-048, JPL, Los Angeles, USA, August 26 1998

Swenson S, Wahr J (2006) Post-processing removal of correlated errors in GRACE data, Geophys. Res. Lett., 33, L08402. doi:10.1029/2005GL025285

Tapley B, Bettadpur S, Watkins M, Reigber C (2004) The gravity recovery and climate experiment: Mission overview and early results, Geophysical Research Letters, 31(2004), L09607. doi:10.1029/2004GL019920

Wahr J, Molenaar M, Bryan F (1998) Time variability of the Earth's gravity field: Hydrological and oceanic effects and their possible detection using GRACE, J. Geophys. Res., 103(B12), 30205–30229, doi:10.1029/98JB02844.

Wickert J, Michalak G, Schmidt T, Beyerle G, Cheng C, Healy S (2009) GPS Radio Occultation: Results from CHAMP, GRACE and FORMOSAT-3/COSMIC, Terresstrial Atmospheric Ocean Science, 20 (2009), 35-50

Wang L, Shum CK, Simons FJ, Tapley B, Dai C (2012) Coseismic and postseismic deformation of the 2011 Tohoku-Oki earthquake constrained by GRACE gravimetry. Geophysical Research Letters, 39:7301. doi:10.1029/2012GL051104

Wouters B, Bonin JA, Chambers DP, Riva REM, Sasgen I, Wahr J (2014) GRACE, time-varying gravity, Earth system dynamics and climate change. Reports on Progress in Physics, vol 77. doi:10.1088/0034-4885/77/11/116801